CONTRACT REPORT BRL-CR-569

AD-A183 798

MODIFICATIONS IN EPIC-2 SUBCYCLING AND QUADRILATERALS
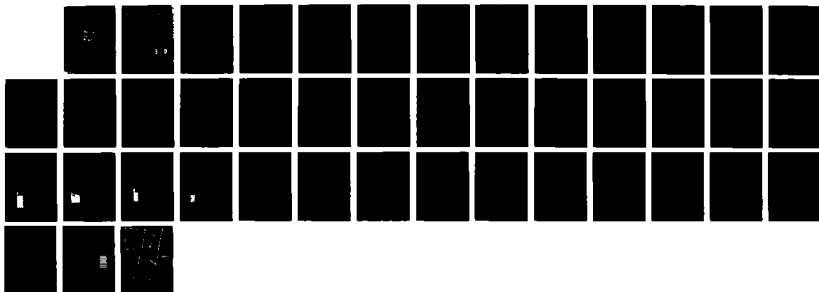
TED BELYTSCHKO, INC.
18 LONGMEADOW ROAD
WINNETKA, IL 60093

JUNE 1987

US ARMY BALLISTIC RESEARCH LABORATORY
ABERDEEN PROVING GROUND, MARYLAND

REPORT DOCUMENTATION PAGE

Form Approved
OMB No 0704-0188
Exp Date Jun 30, 1986

1a. REPORT SECURITY CLASSIFICATION	1b. RESTRICTIVE MARKINGS
Unclassified	None

2a. SECURITY CLASSIFICATION AUTHORITY	3. DISTRIBUTION / AVAILABILITY OF REPORT
2b. DECLASSIFICATION / DOWNGRADING SCHEDULE	

4. PERFORMING ORGANIZATION REPORT NUMBER(S)	5. MONITORING ORGANIZATION REPORT NUMBER(S)

6a. NAME OF PERFORMING ORGANIZATION	6b. OFFICE SYMBOL (If applicable)	7a. NAME OF MONITORING ORGANIZATION
Ted Belytschko Inc.		Ballistic Research Laboratory

6c. ADDRESS (City, State, and ZIP Code)	7b. ADDRESS (City, State, and ZIP Code)
18 Longmeadow Rd. Winnetka, IL 60093	Aberdeen Proving Ground, Maryland 21005-5066

8a. NAME OF FUNDING / SPONSORING ORGANIZATION	8b. OFFICE SYMBOL (If applicable)	9. PROCUREMENT INSTRUMENT IDENTIFICATION NUMBER
		DAAG29-81-D-0100

8c. ADDRESS (City, State, and ZIP Code)	10. SOURCE OF FUNDING NUMBERS			
	PROGRAM ELEMENT NO.	PROJECT NO.	TASK NO.	WORK UNIT ACCESSION NO
	612618			

11. TITLE (Include Security Classification)

Modifications in EPIC-2 Subcycling and Quadrilaterals

12. PERSONAL AUTHOR(S)
Belytschko, Theodore Bohdan; Lin, Jerry I.; Jonas, George Herbert*

13a. TYPE OF REPORT	13b. TIME COVERED	14. DATE OF REPORT (Year, Month, Day)	15. PAGE COUNT
Final	FROM March 82 to July 86		

16. SUPPLEMENTARY NOTATION

*U. S. Army Ballistic Research Laboratory

17. COSATI CODES			18. SUBJECT TERMS (Continue on reverse if necessary and identify by block number)
FIELD	GROUP	SUB-GROUP	EPIC-2 Penetrators Hourglass Control Impact
20	14		Finite Elements; Explicit-Explicit Ballistics
19	4		Subcycling

19. ABSTRACT (Continue on reverse if necessary and identify by block number)

The following modifications of the code EPIC-2 are described: (1) subcycling, which permits different time steps to be used in different parts of the mesh; (2) the addition of a four-node quadrilateral which uses one quadrature point and employs a consistent hourglass control and (3) a rigid interface to interconnect meshes with different element sizes. Both the theoretical and programming aspects are described.

20. DISTRIBUTION / AVAILABILITY OF ABSTRACT	21 ABSTRACT SECURITY CLASSIFICATION
☒ UNCLASSIFIED/UNLIMITED ☐ SAME AS RPT ☐ DTIC USERS	Unclassified

22a NAME OF RESPONSIBLE INDIVIDUAL	22b TELEPHONE (Include Area Code)	22c OFFICE SYMBOL
George H. Jonas	(301) 278-6083	SLCBR-TB-P

DD FORM 1473, 84 MAR

83 APR edition may be used until exhausted
All other editions are obsolete

The following page is blank.

TABLE OF CONTENTS

LIST OF FIGURES

iii

1. INTRODUCTION

This report describes three new features which have been incorporated in the EPIC-2 [1] code:

1. Subcycling, which permits different time steps to be used in different parts of the mesh.

2. A four-node quadrilateral which uses one quadrature point and employs a consistent control of the hourglass modes.

3. A rigid interface which can be used to connect meshes with different elements sizes.

As has been succinctly summarized by Zukas [2] in his survey of computer methods for impact and penetration, "computational techniques have advanced to the point where extremely difficult situations can be analyzed quickly . . . one dimensional problems in tens of minutes to a few hours, and three dimensional problems in a few hours to tens of hours." With the decreasing costs of computers, these figures, which apply to the larger main-frame computers, promise to diminish rapidly. Nevertheless, it is quite clear that we are still far from the stage where even two-dimensional calculations can be used effectively in the design and decision-making process, since the parametric studies which are essential in such highly nonlinear simulations simply cannot be made within the normal framework of engineering time schedules because of their long running times.

However, substantial savings in computer time can be achieved in these programs through improvements of the time integration process and element technology. Even relatively simple techniques such as those described here can lead to reductions of computer time by factors of as much as 3 to 10 for two-dimensional calculations, reductions as large as 10 to 20 for three-

1

dimensional calculations. These savings promise to be important not only in the use of such programs on large main-frame computers, but on smaller computers, where they may make these calculations feasible.

In the next section, we review alternative integration methods and two methods of multi-time-step explicit time integration (explicit-explicit partition) and describe our reasons for the choice of the method that has been programmed into the EPIC-2 code. We then describe the actual programming steps in more detail and the procedures for using this multi-time step logic. The explicit-explicit algorithm permits an almost arbitrary number of different time steps to be used throughout the mesh, as long as the ratio of time steps between adjacent elements are integer multiples of each other. It also permits the time steps to be varied and calculated automatically, which is a development which we have not seen reported for any other program.

A 4-node quadrilateral element [3] has been added in EPIC-2 to provide an alternative to the triangular element. Four-node quadrilaterals with one-point quadrature provide more efficient computations because they require fewer constitutive evaluations and converge faster because they are not as stiff as triangles; triangular elements tend to lock for incompressible materials unless special arrangements of elements are used. However, the one-point quadrature element possesses spurious singular modes known as hourglass modes. To control these modes, a consistent hourglass control procedure first described in Ref. [3] is used. Both this element and the existing triangular element are programmed to accommodate the explicit-explicit time integration scheme. The implementation of this quadrilateral element is stated in Section 4.

The rigid interface provides a technique for combining meshes with different element sizes without any intermediate elements. It enhances the

2

efficiency of the subcycling technique because it increases the differences in the critical time steps of different element groups. When previous versions of the EPIC-2 mesh generator were used, the critical time step of different element size groups did not vary much, so subcycling was quite ineffective. This rigid interface is described in Section 5.

2. RATIONALE FOR CHOICE OF TIME INTEGRATION METHOD

We will write the governing equations for the finite element semidiscretization in the form

$$M \ddot{u} = f \tag{2.1}$$

where M is an assembled mass matrix which is considered to be lumped and hence diagonal, u is the matrix of nodal displacements, superposed dots denote time derivatives, and f is a column matrix of nodal forces which is given by

$$f = f_{ext} - f_{int} \tag{2.2}$$

In the central difference method with a changing time step, these equations are integrated by updating the nodal velocities and displacements with the following formulas

$$\dot{u}^{n+1/2} = \dot{u}^{n-1/2} + \overline{\Delta t}^{\,n} (M^{-1} f^n) \tag{2.3}$$

$$u^{n+1} = u^n + \Delta t^n \dot{u}^{n+1/2} \tag{2.4}$$

3

$$\Delta \overline{t}^n = \frac{1}{2} (\Delta t^n + \Delta t^{n-1}) \qquad (2.5)$$

where Δt is the time increment and superscripts denote the step number. The time increment Δt is limited for stability by the requirement

$$\Delta t_{crit} < \frac{2}{\omega_{max}} [(1 + \mu_d^2)^{1/2} - \mu_d] \qquad (2.6)$$

where ω_{max} is the maximum natural frequency in the finite element mesh and μ_d is the fraction of critical damping in this frequency. The formulas of Flanagan and Belytschko [3] may be used to show that the maximum frequency of a uniform strain element is bounded by

$$\omega_{max} < \max_{for\ all\ e} \frac{4(\lambda + 2\mu)}{\rho A^2} \sum_{i=1}^{2} \sum_{I=1}^{N} B_{iI} B_{iI} \qquad (2.7)$$

where λ and μ are the Lame constants, ρ the density, N is the number of nodes for each element, A the area of the element and B_{iI} are the components of the strain-displacement matrix which relate the velocity gradients to the nodal velocities by

$$\dot{u}_{i,j} = \sum_{I=1}^{N} B_{jI} \dot{u}_{iI} \qquad (2.8)$$

Although in [3] this formula is only given in this form for quadrilaterals, it has been recently shown that it also applies to triangles. By using the standard expressions for the elements of the $\underset{\sim}{B}$ matrix, and for the dilatational wave speed, which is

4

$$c_p^2 = \frac{\lambda + 2\mu}{\rho} \tag{2.9}$$

it can be shown that this formula gives the following constraint on the
maximum frequency

$$\omega_{max}^2 > \frac{4c_p^2 s^2}{A^2} \tag{2.10}$$

where s is a characteristic length of the element. For a triangle, s is the
length of the longest side. Using the Rayleigh's theorem, it can be shown
that the maximum mesh frequency is always bounded from above by the maximum
element frequency. For an undamped system, Eqs. (6) and (10) can be shown to
bound the time step by

$$\Delta t_{crit} < \frac{A}{sc_p} \tag{2.11}$$

which for a right-triangle gives

$$\Delta t_{crit} < \frac{h_{min}}{2\,c_p} \tag{2.12}$$

where h_{min} is the distance from the node at the right angle to the hypotenuse.

Equation (12) differs from the formula used in EPIC-2 by the factor 2
in the denominator. This formula is only a lower bound, so it cannot be said
with certainty that a computation which omits this factor would necessarily be
unstable, but our work indicates that in general the omission of this factor
may lead to any unconservative estimate of the stable time step.

Nevertheless, the important point which is made by Eqs. (11) and (12) is
that the stable time step depends on the dimension of the element and de-

5

creases as the size of the element decreases. Therefore in penetration cal-
culations, where the elements adjacent to the penetrator are severely com-
pressed, the stable time step is drastically reduced. This leads to the main
drawback of single-step, explicit integration where the entire mesh must then
be integrated with this very small time step.

Several new methods have been devised for circumventing this difficulty
of single time step integration. Belytschko and Mullen [4], [5] have presen-
ted an explicit-implicit partition where part of the mesh is integrated
implicitly, and the rest is integrated explicitly. They have shown that the
stability limit on the time step is then determined strictly by the highest
frequency in the explicit partition, or in other words, that Eq. (6), and the
resulting Eqs. (11) and (12), need only be met in the part of the mesh that is
integrated explicitly.

At first glance, this would seem to offer substantial benefits in the
penetration problem, for by integrating the highly compressed zones next to
the penetrator implicitly, the severe reduction in the stable time step which
is caused by the squashing of these elements would be avoided. However, the
difficulty in applying this to the penetration problem is that the zones which
are compressed are adjacent to the slide line. Integrating these nodes
implicitly has the following drawbacks:

1) it is difficult to formulate a stiffness matrix for the slide line
because of the constant realignment of nodes which takes place;

2) slide lines tend to malfunction if a large time step is used.

An alternative explicit-implicit partition has been developed by Hughes
and Liu [6] and recently extended by Liu and Belytschko [7] to multi-time step
explicit-implicit partitions, where different time steps can be used in con-
junction with the mesh partitioning. This would appear to have substantial

6

potential in the penetration problem in that the implicit integrator could be used in all zones close to the penetrator except for those directly on the slide line. The elements connected to the slide line could then be integrated with a very small time step and an explicit integrator. Although this alternative is quite appealing, it was ruled out for the following reasons:

1) we have had very little experience with the application of this method in structural dynamics; the problems which have been tried by this method have been primarily heat conduction problems which tend to be inherently more stable;

2) the implementation of this procedure would require the development of a stiffness matrix and hence considerable recoding.

The extensive recoding which would be required makes this alternative quite unattractive. The code structure of explicit-implicit codes is inherently quite different from purely explicit codes, so that the introduction of the implicit option without complete recoding would be very difficult.

Another alternative to overcoming the drawbacks of conditional stability is to use different time steps in different parts of the mesh. This procedure was studied in [8], where it was shown that if linear interpolation is used on the displacements of the interface nodes, the procedure is conditionally stable provided Eq. (6) is satisfied for each node and ω_{max} is the lowest maximum frequency of any element connected to the node. In [9] it was shown that this procedure is equivalent to a constant velocity interpolation, which is easier to program; [10] describes the implementation of this method in the code SAMSON 2.

Explicit/explicit partitions have also been discussed by Wright [11] but no details on the implementation were given. For these reasons, the explicit/explicit partition first investigated in [8] and further developed in [9] and [10] was implemented in EPIC-2.

7

3. EXPLICIT-EXPLICIT PARTITION IN EPIC-2

The procedure used in modifying EPIC-2 is based on an explicit-explicit partitioning procedure, or subcycling procedure, presented in [10]. In this method, the elements are separated into element groups, each of which can be integrated with a different time step subject to the following restrictions:

1. All time steps must be integer multiples of the smallest time step.

2. If any node is shared by elements in two different integration groups, the time steps in these groups must be integer multiples of each other.

The time step for each element group is recomputed at the end of the total cycle but kept constant during the subcycles. All elements near the slave nodes must be included in element group 1 to ensure that the slide line is always integrated by the minimum time increment. If the smallest time step does not belong to element group 1, the run stops automatically. No additional requirement for the arrangement of element group numbers is necessary. The elements adjacent to the master nodes can be marked by group number other than 1. As soon as the slide line interaction is detected, the group indicator for the elements involved will be checked and designated to be 1. This is equivalent to an expanding interaction zone in the target and thus avoids integrating the elements that are not engaged in interaction by an unnecessarily small time step.

For purpose of defining how the explicit-explicit partitioning procedure works, we will define the following variables.

NTGRP: number of groups into which the finite element mesh is subdivided

Δt_G: the time increment for element group G

t_M : the master time

Δt_M: the master time increment, which corresponds to the minimum Δt_G among all element groups G

As stated previously, all element time step increments Δt_G must be integer multiples of Δt_M. The maximum Δt_G is called Δt_{max}.

The program is designed so that it automatically decides the appropriate nodal time step. This is accomplished by using the largest time increment for any element group connected to the node to update the node. In order to program this algorithm, each node therefore requires two additional words of storage: the nodal time t_N and the time increment used for that node, Δt_N.

The essence of the procedure is as follows. We call the time steps necessary to advance the master clock by Δt_{max} a cycle. Within a cycle, whenever the master clock t_M is incremented by Δt_M, all elements are first checked. If any element is in a group which is not ahead of the master time, i.e. if element I is in group G and

$$t_G < t_M \qquad\qquad (3.1)$$

that element is updated. This updating involves the calculation of new velocity strains, stresses and internal forces. The element internal forces are then added into the global internal force matrix.

After all elements have been updated, the nodal loop for updating velocities and displacements is executed. In this loop, prior to updating the velocities and displacements, the nodal clock t_N is checked. If

9

$$t_N < t_M \qquad\qquad (3.2)$$

the nodal clock is behind the master clock, so the node is updated. In addition, the nodal clock is updated using the time increment for that node.

The algorithm assumes that a velocity strain formulation is used for all element calculations. When an element needs to be updated, the latest available velocity is used to compute the velocity strain. This means if an element is connected to a node with a larger time step, it uses the same nodal velocity for all intermediate time steps. This corresponds to a constant velocity interpolation or a linear displacement interpolation, which experience has shown to be stable. A flow chart for the procedure is shown in Table 1.

An important characteristic of impact/penetration calculations is that the nodes on the sliding interface cannot be updated with a Courant number of 1. Instead a substantially smaller time step, such as $0.2 \, \Delta t_{crit}$ to $0.5 \, \Delta t_{crit}$ should be used. This restriction is necessary because the velocity adjustment algorithms which are used to enforce compatibility on a slideline fail if the nodes penetrate too far into an element during a time step. Therefore, in EPIC-2 the elements with any nodes on the slide line are automatically allocated to the element group with the smallest time step.

Table 1

Flowchart of Explicit-Explicit Partition

1. Set initial condition

$$\underset{\sim}{u}^0 = \underset{\sim}{u}(o) \; , \qquad \underset{\sim}{u}^{-1/2} = \underset{\sim}{\dot{u}}(o)$$

   initial accelerations are assumed to vanish $\underset{\sim}{\ddot{u}}^0 = 0.$

2. Initialize clocks and cycle counters

   $t_M \quad = 0 \; ; \quad$ master time

   $t_G \quad = 0 \qquad$ for all element groups G

   $t_N \quad = 0 \qquad$ for all nodes N

   $n \quad = 0$

   $n2_{max} = 1$

3. Set up nodal time step and subcycle counter

   $n2 \quad = 0$

   $\Delta t_N \quad = \max_G (\Delta t_G)$ for all nodes N . G represents any element group connected to node N.

4. Update nodes behind master clock

   a. DO N = 1 to NNODE

   b. if $t_N > t_M$, skip node N

   c. new accelerations $\underset{\sim}{\ddot{u}}_N^{n+1} = \underset{\sim}{M}^{-1} \underset{\sim}{f}$

   d. update nodal velocities: $\underset{\sim}{\dot{u}}_N^{n+1/2} = \underset{\sim}{\dot{u}}_N^{n-1/2} + \overline{\Delta t}_N \, \underset{\sim}{\ddot{u}}_N^n$

   e. update nodal displacements: $\underset{\sim}{u}_N^{n+1} = \underset{\sim}{u}_N^n + \Delta t_N \, \underset{\sim}{\dot{u}}_N^{n+1/2}$

   f. update nodal clock: $t_N \leftarrow t_N + \Delta t_N$

11

5. Compute internal forces $f_{\sim int}^{n+1}$

    a. zero $f_{\sim}^{int}$

    b. DO N = 1 to NELE

    c. if $t_G > t_M$, skip element N (element N belongs to group G)

    d. compute velocity strains: $D_{\sim N}^{n+1/2} = B_{\sim}\, \dot{u}_{\sim N}^{n+1/2}$

    e. compute stress increments $\dot{T}_{\sim N}^{n+1/2}$ by the constitutive relations

    f. update stress: $T_{\sim N}^{n+1} = T_{\sim N}^{n} + \Delta t_G\, \dot{T}_{\sim N}^{n+1/2}$

    g. compute element internal forces: $f_{\sim int,N}^{n+1} = \int_{V_N} B_{\sim}^{T}\, T_{\sim N}^{n+1}\, dV$

    h. if n2 = 1, compute stable time increment for element

    i. assemble $f_{\sim int,N}^{n+1}$ into $f_{\sim int}^{n+1}$

    j. update element group clock: $t_G \leftarrow t_G + \Delta t_G$

6. compute $f_{\sim}^{ext}$

7. update master clock and cycle counters

    $t_M \leftarrow t_M + \Delta t_M$

    $n \leftarrow n + 1$

    $n2 \leftarrow n2 + 1$

8. if $n2 = n2_{max}$, set new element group time increment Δt_G, $n2_{max} = 1$ and go to 3; otherwise go to 4.

4. CONSTANT STRAIN QUADRILATERAL WITH HOURGLASS CONTROL

An underintegrated 4-node quadrilateral element with orthogonal hourglass contról, proposed in [3] by Flanagan and Belytschko, has been added to the EPIC-2 program. The element is adapted for both plane strain and axisymmetric cases. It not only reduces the number of elements by half against a triangular element mesh with the same amount of nodes, but also permits a

12

greater stable time step.

The related equations for this element can be found in Ref. [3]. A concise and efficient computational procedure is summarized by Belytschko et al. in [12].

In the new version of EPIC-2, the implementation of the constant strain quadrilateral element is as following:

1. Set up the discrete gradient operator $\underset{\sim}{B}$ such that $B_{iI} = N_{I,i}$ (evaluated at the quadrature point). The lower case subscript runs from 1 to 2 and represents r and z spatial coordinates, respectively. The upper case subscript has a range of 1 to 4 and represents the nodes of an element.

$$\underset{\sim}{B} = \frac{1}{2A}\begin{bmatrix} z_{24} & z_{31} & z_{42} & z_{13} \\ r_{42} & r_{13} & r_{24} & r_{31} \end{bmatrix} \tag{4.1a}$$

$$z_{IJ} = z_I - z_J \tag{4.1b}$$

$$r_{IJ} = r_I - r_J \tag{4.1c}$$

$$A = (r_{31} z_{42} - r_{42} z_{31})/2 \tag{4.1d}$$

2. Form the velocity gradient

$$\dot{u}_{i,j} = N_{I,j} \dot{u}_{iI} = (\dot{u}_{i1} - \dot{u}_{i3})B_{j1} + (\dot{u}_{i2} - \dot{u}_{i4})B_{j2} \tag{4.2}$$

Note that $B_{j3} = -B_{j1}$ and $B_{j4} = -B_{j2}$.

3. Designate the mean radius for an element

$$\bar{r} = (A_1 \bar{r}_1 + A_2 \bar{r}_2)/(A_1 + A_2) \qquad (4.3a)$$

where

$$A_1 = r_{21} z_{31} - r_{31} z_{21} \qquad (4.3b)$$

$$A_2 = r_{31} z_{41} - r_{41} z_{31} \qquad (4.3c)$$

$$\bar{r}_1 = (r_1 + r_2 + r_3)/3 \qquad (4.3d)$$

$$\bar{r}_2 = (r_1 + r_3 + r_4)/3 \qquad (4.3e)$$

4. Calculate the strain and spin rate

$$\dot{\epsilon}_{ij} = \frac{1}{2} (\dot{u}_{i,j} + \dot{u}_{j,i}) \qquad (4.4a)$$

$$\dot{\omega}_{ij} = \frac{1}{2} (\dot{u}_{j,i} - \dot{u}_{i,j}) \qquad i \neq j \qquad (4.4b)$$

and the additional strain component

$$\dot{\epsilon}_{\theta\theta} = (\sum_I \dot{u}_{rI})/(4\bar{r}) \qquad \text{for axisymmetric case only.} \qquad (4.5)$$

5. Compute $\dot{\sigma}_{rr}$, $\dot{\sigma}_{zz}$, $\dot{\sigma}_{rz}$ and $\dot{\sigma}_{\theta\theta}$ based on constitutive law and Von Mises yield criterion. This step remains unchanged as it is in subroutine STRESS of the original EPIC-2 program

14

6. Set up $\underset{\sim}{H} = \begin{bmatrix} H_r \\ H_z \end{bmatrix} = \begin{bmatrix} h_I r_I \\ h_I z_I \end{bmatrix}$ (4.6a)

where

$$\underset{\sim}{h}^T = [1\ -1\ 1\ -1]$$ (4.6b)

and the hourglass strain rate

$$q_i = h_I \dot{u}_{iI} - H_j \dot{u}_{i,j}$$ (4.7)

7. Update the hourglass stress

$$Q_i = Q_i^{t-\Delta t} + \Delta t\ (\kappa B_{jJ}\ B_{jJ}\ q_i - \dot{\omega}_{ij}\ Q_j^{t-\Delta t})$$ (4.8)

here κ is a user-controlled parameter which determines how much resistance would be added. The recommended range for κ is from 0.01 to 0.1.

8. Compute the nodal force

$$f_{iI} = V\ [B_{jI}(\sigma_{ij} - H_j Q_i) + h_I Q_i + \frac{\sigma_{\theta\theta}}{4\bar{r}}]$$ (4.9)

for plane strain element $V = A$ and $\sigma_{\theta\theta} = 0$;

for axisymmetric element $V = 2\pi\bar{r}A$

15

Program Implementation

Two additional subroutines, QSTRN and QFINT, were programmed in the latest version of EPIC-2. They are corresponding to the calculation of velocity strains and internal forces for the quadrilateral element respectively.

The major modifications for the explicit-explicit subcycling integration scheme were made in subroutine LOOP. We will first define the primary variables in these modifications, then define what size these arrays need to be in Table 2.

Major Variables

DTNOD(N) . . . time increment for node N, Δt_N

DTNODO(N) . . . previous time increment for node N

CLKNOD(N) . . . clock time for node N, t_N

DTGRP(NG) . . . time increment for element group N^G, Δt_{NG}

DTGRPO(NG). . . previous time increment for element group NG

CLKGRP(N) . . . clock time for element group N^G

NEGRP(N) . . . integration group number for element N; if NEGRP(N) = J, element N will be integrated with time increment Δt_J

TIME   =   master time t_M

NCYC2   =   subcycle counter, n2 in flow chart

N2LIM   =   number of subcycles in cycle

NTGRP   =   number of element groups

NNODE*   =   number of nodes

NELE*   =   number of elements

* already exist in program

Table 2

Minimum Array Size in COMMON Statement

of Variables

Variable	Minimum Size
DTNOD	NNODE
DTNODO	NNODE
CLKNOD	NNODE
DTGRP	NTGRP
DTGRPO	NTGRP
NEGRP	NELE
CLKGRP	NTGRP

5. RIGID INTERFACE ALGORITHM

In order to conserve computational effort, the mesh generator in EPIC-2 has the capability of increasing the element size for those elements away from the domain of interest, namely, the impact zone. This mesh gradation as it is implemented in EPIC-2 is illustrated in Fig. 1a; region A represents the domain of interest. For a uniform material, this type of mesh gradation results in little difference in the critical time step among the element groups since the shortest side of the element governs the time step and it is of approximately the same length in the three groups of elements. The advantage of the explicit subcycling scheme, which depends on the differences on critical time steps between element groups, is therefore quite minimal with this element
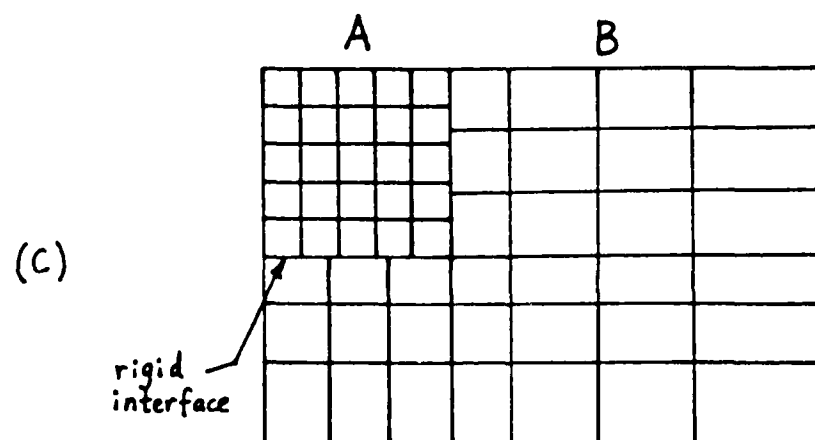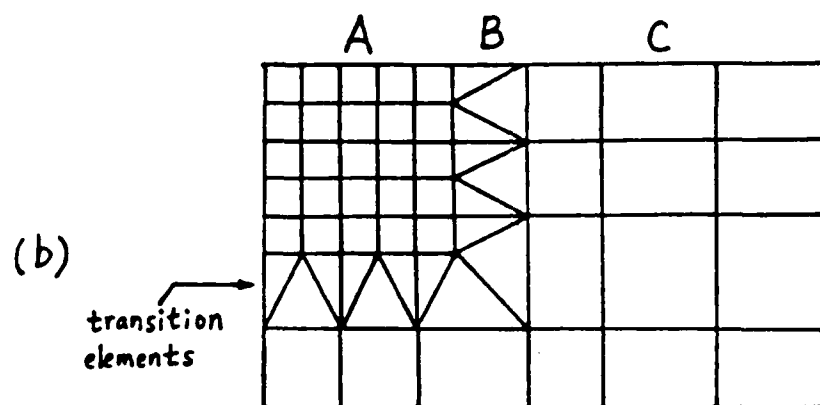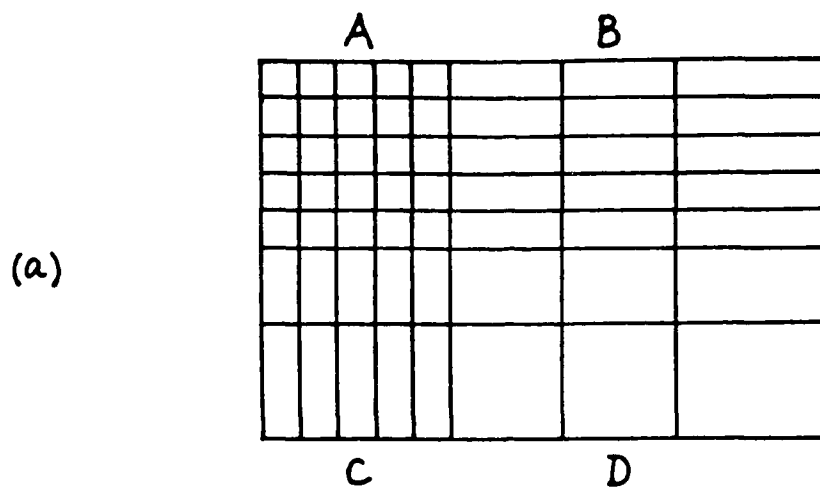
17

Figure 1.   Schematic of mesh gradations for penetration problems.

gradation scheme.

To take advantage of subcycling, it is necessary to construct meshes with gradations in element size that retain nearly square elements. Unfortunately, this requires a layer of transition elements between element groups as shown in Fig. 1b. However, this usually causes severe inconvenience in generating data. To avoid these difficulties, a rigid interface algorithm was developed. Two dissimilar meshes are allowed to meet on the rigid interface as shown in Fig. 1c.

We designate the nodes on the coarse mesh side of the rigid interface as primary nodes and those on the fine mesh side as secondary nodes. The primary nodes and secondary nodes are marked by P and S respectively in Fig. 2. Sometimes a primary node and a secondary node may share the same position in the space, however they are considered distinctive nodes in this algorithm.

The ground rules of this algorithm are:

i) the primary nodes can move independently;

ii) the secondary nodes must respond accordingly, in a manner which minimizes the violation of compatibility, to the movement of the adjacent primary nodes.

The secondary nodes are constrained to remain on the line connecting two adjacent primary nodes. Full compatibility is then maintained only if the ratios of the sides of adjacent elements are integer multiples. However, when the ratio is not an integer mutiple, as in Fig. 1c, the deviations from compatibility are insignificant.

The procedure for the rigid interface algorithm is as follows:

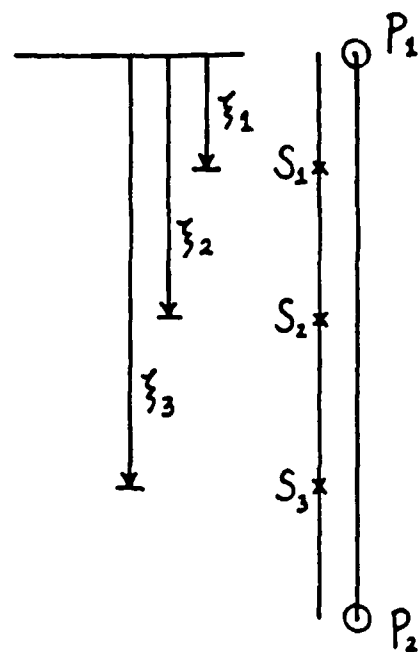Step 1. Set up the non-dimensionalized natural coordinates ξ_i for all secondary nodes. We define

Figure 2. **Primary nodes and secondary nodes on a rigid interface.**

$$\xi_i = \frac{|\underset{\sim}{x}_S^i - \underset{\sim}{x}_P^1|}{|\underset{\sim}{x}_P^2 - \underset{\sim}{x}_P^1|} \qquad i = 1 \text{ to } NS \qquad (5.1)$$

where NS is the number of secondary nodes between primary nodes P_1 and P_2, $\underset{\sim}{x}$ represents the position vector for a node and $|\;\;|$ denote the magnitude of a vector. Subscripts P and S refer to primary and secondary nodes, respectively. Superscripts denote the node number. An example for the natural coordinate ξ_i is illustrated in Fig. 2.

Step 2. Distribute the lumped mass of the secondary nodes to the adjacent primary nodes.

$$M_P^1 = m_P^1 + \sum_{i=1}^{NS} (1 - \xi_i)m_S^i \qquad (5.2a)$$

$$M_P^2 = m_P^2 + \sum_{i=1}^{NS} \xi_i \, m_S^i \qquad (5.2b)$$

where m_P^i and m_S^i are the original masses from the assembly operation, and M_P^i is the adjusted mass for primary node P_i.

Remark: Steps (1) and (2) a.e executed before entering the integration loop since, as will be seen later, the natural coordinates ξ_i remain constants throughout the run.

Step 3. Compute the accelerations, velocities and displacements of all the nodes except the secondary nodes in the regular manner. The adjusted mass M_P^i, instead of the original mass m_P^i, must be used for updating the primary node velocity, i.e.

$$(\underset{\sim}{v}_P^i)^{t + \frac{\Delta t}{2}} = (\underset{\sim}{v}_P^i)^{t - \frac{\Delta t}{2}} + (M_P^i)^{-1} \underset{\sim}{f}^t \, \Delta t \qquad (5.3)$$

21

Step 4. Enforce the rigid interface constraint on the velocity $\underset{\sim}{v}_S^i$ based on $\underset{\sim}{v}_P^1$ and $\underset{\sim}{v}_P^2$ of the adjacent primary nodes P_1 and P_2.

$$\underset{\sim}{v}_S^i = (1 - \xi_i)\underset{\sim}{v}_P^1 + \xi_i \underset{\sim}{v}_P^2 \qquad \text{(loop over secondary nodes i)} \qquad (5.4)$$

Then the displacement $\underset{\sim}{d}_S^i$ is updated in the usual way.

Step 5. No modification is needed in the element calculations. After all nodal forces are determined, the nodal forces on secondary nodes are transferred onto the adjacent primary nodes.

$$\underset{\sim}{f}_p^1 + \underset{\sim}{f}_p^1 + (1 - \xi_i)\underset{\sim}{f}_S^i \qquad (5.5a)$$

(loop over secondary nodes i)

$$\underset{\sim}{f}_p^2 + \underset{\sim}{f}_p^2 + \xi_i \underset{\sim}{f}_S^i \qquad (5.5b)$$

Since the displacement between two adjacent primary nodes is linear and a linear interpolation is used in step (4) to determine the secondary node velocity, the natural coordinates for secondary nodes will remain constants. This corresponds with our remark in step (2).

Two runs with the rigid interface have been examined. The original and deformed models are shown in Figs. 3. and 4. No numerical instability has been detected in either case.
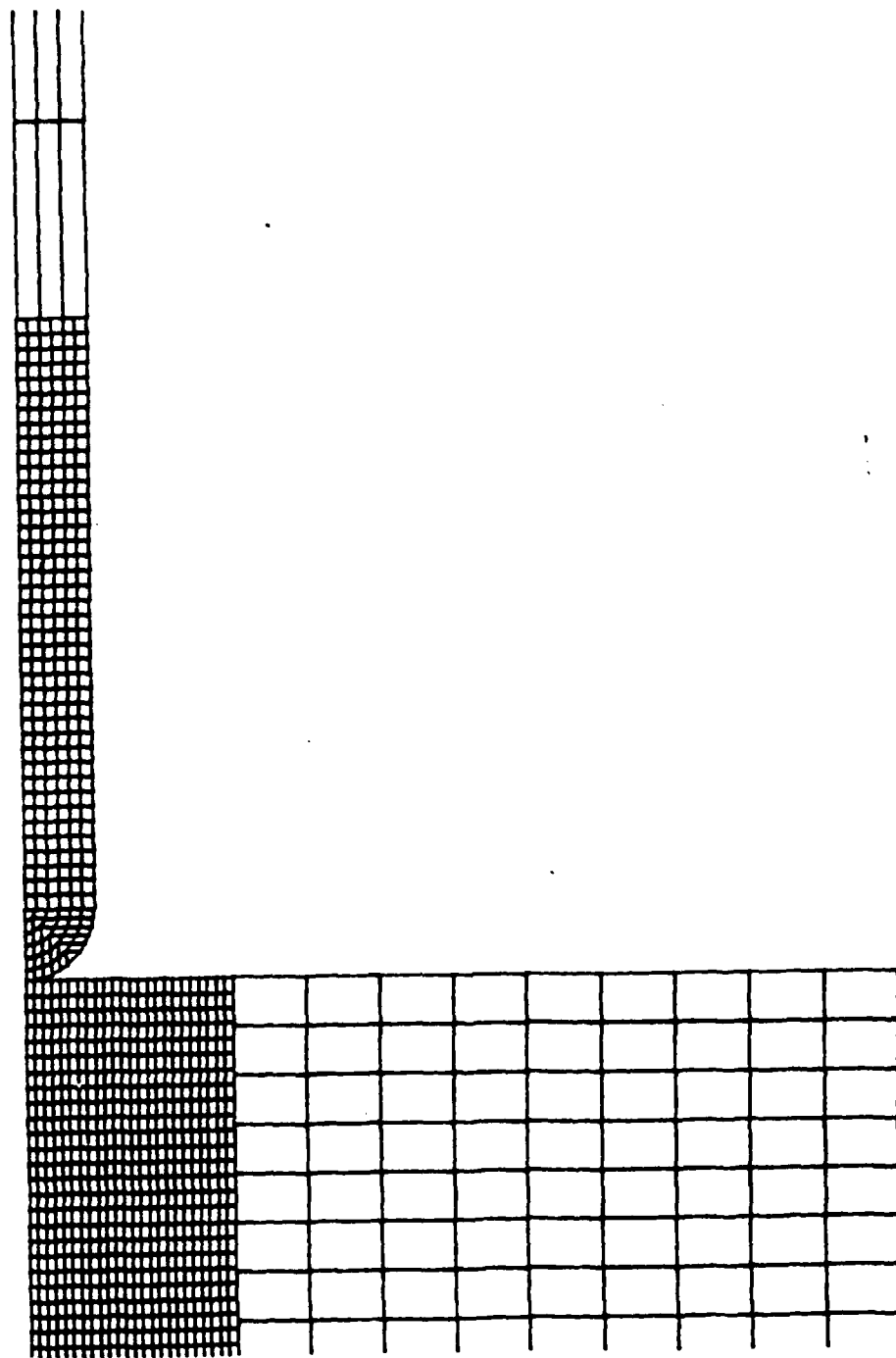
Figure 3a. Example 1 for a subcycling run with rigid interfaces.
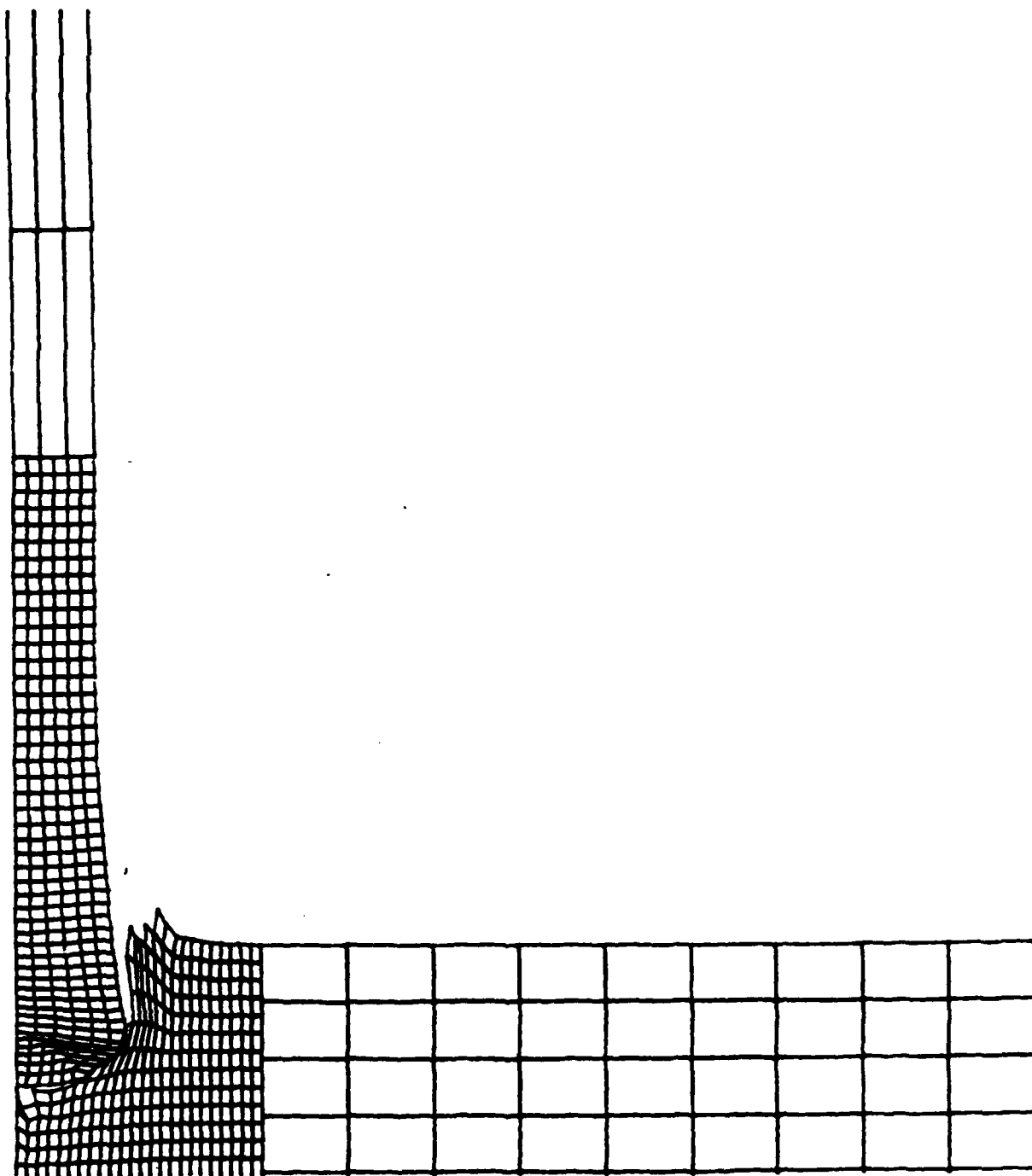
23

Figure 3b. Example 1 for a subcycling run with rigid interfaces.
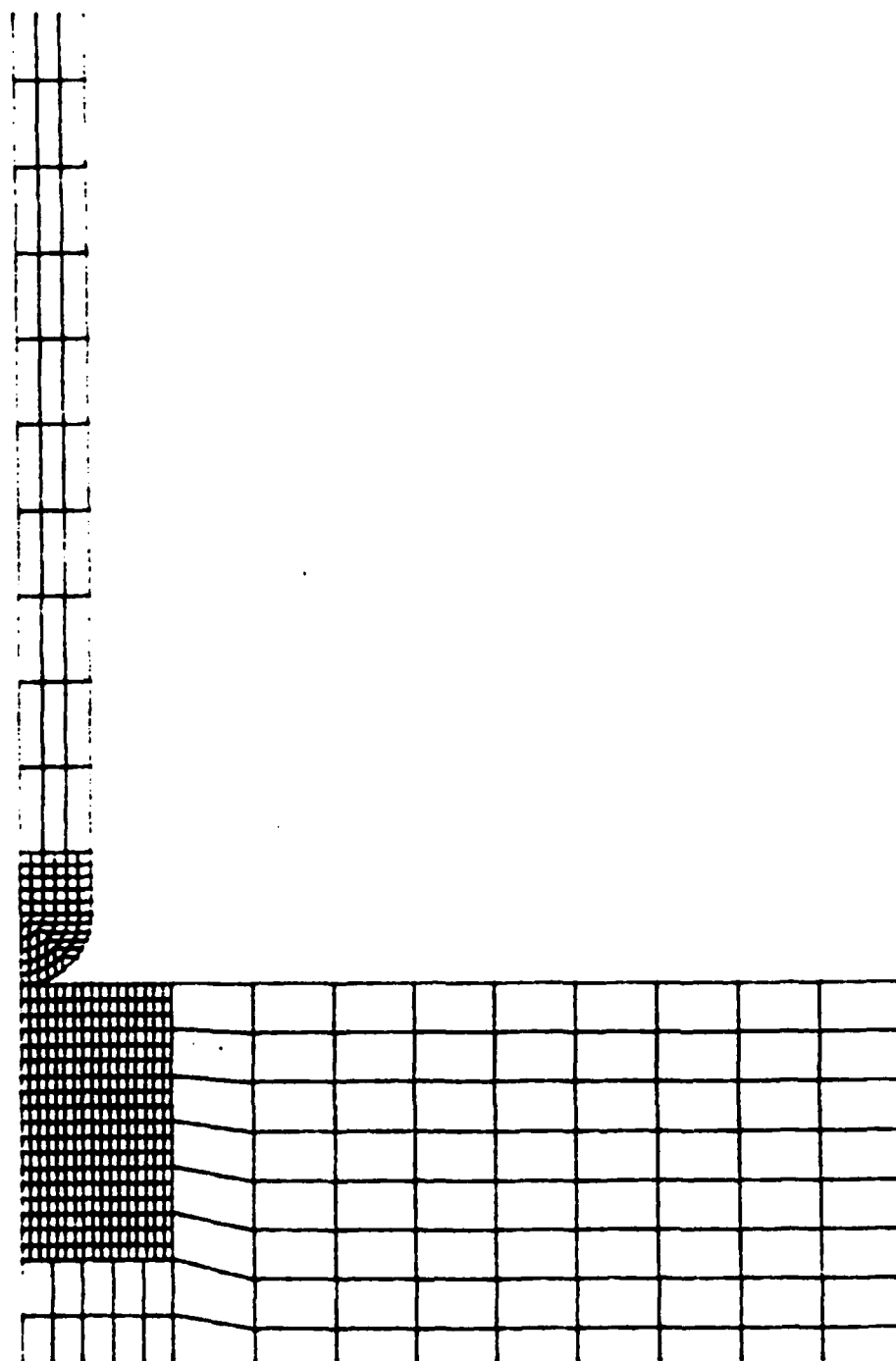
24

Figure 4a. Example 2 for a subcycling run with rigid interfaces.
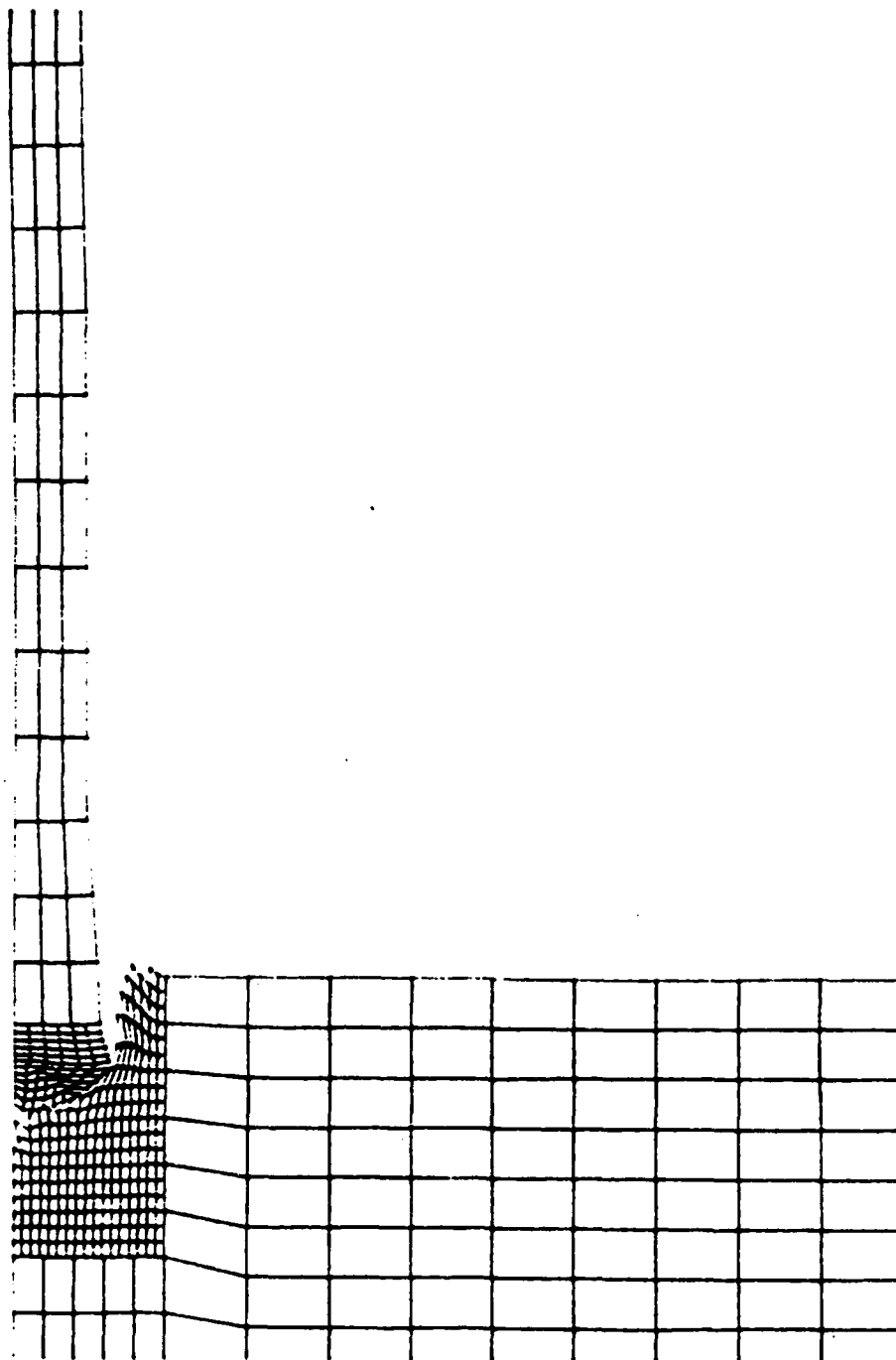
Figure 4b. <u>Example 2 for a subcycling run with rigid interfaces</u>.

6. INPUT CHANGES

The following additions in input are necessary to run this modified version of EPIC-2.

Solid Material Cards (5E15.8) - Add one additional parameter HRCON for each material. HRCON is the hourglass control factor for quadrilaterals (0.05 to 0.2 is recommended).

Miscellaneous Card (7I5) - Add one additional parameter NTGRP in column 36-40. NTGRP is the number of groups into which the finite element mesh is subdivided.

Element Data Cards (10I5) - Add one additional parameter NETYPE in column 46-50. NETYPE is set to one for quadrilaterals, otherwise equal to zero or blank.

Special Shapes Element Data Cards (8I5) - Add one additional parameter NETYPE (0 or 1) in column 36-40.

Element Group Array for Subcycling (5I5) - The parameters are IGRP, KG1, KG2, KG3 and KG4. For each element group there should be at least one card. This group of cards is followed with a blank card to flag that all element groups are completed. This group of cards is inserted right after all element cards and blanks. IGRP is the number of the element groups whereas KG1, KG2 and KG3 are indices of DO loops and KG4 is an interval. This can best be explained with an example. Consider the elements 1 to 20 and that they represent two element groups. The first being 1,2 6 ,7 11,12 16,17 and the second 3,4,5 8,9,10 13,14,15 18,19,20. The first element group would have KG1=1 and KG2=2 where 1 and 2 are the first and last entry in the first set. KG4=5 is the interval between 1 and 6 and KG3=3 the number of sets less one. The second element group would have KG1=3 and KG2=5 and an interval of KG4=5 (difference of 3 and 8) and again KG4=3.

Rigid Interface Card (I5)

This card follows the regular slideline cards

column	variable name	description
1 - 5	NRSL	number of rigid interfaces to be read in.

Number of Primary and Secondary Nodes (2I5)

column	variable name	description
1 - 5	NMNO	number of primary nodes for this rigid interface

6 - 10	NSNO	number of secondary nodes for this rigid interface

Primary Nodes for Rigid Interface (16I5)

column	variable name	description
1 - 5	IMNO(1)	primary node numbers
6 - 10	IMNO(2)	
etc.		

Secondary Nodes for Rigid Interface (16I5)

column	variable name	description
1 - 5	ISNO(1)	secondary node numbers
6 - 10	ISNO(2)	
etc.		

These last three sets are repeated NRSL number of times.

REFERENCES

1. Johnson, G.R., "EPIC-2, A Computer Program for Elastic-Plastic Impact Computations in 2 Dimensions Plus Spin," Ballistic Research Laboratory, Report ARBRL-CR-00373, June 1978.

2. Zukas, J.A., et al., "Impact Dynamics," John Wiley and Sons, New York, 1981, Chapter 10.

3. Flanagan, D.P. and Belytschko, T., "A Uniform Strain Hexahedron and Quadrilateral with Orthogonal Hourglass Control," Intl. Journal for Numerical Methods in Engineering, Vol. 17, 1981, pp. 679-706.

4. Belytschko, T. and Mullen, R., "Mesh Partitions of Explicit-Implicit Time Integration," Formulations and Computational Algorithms in Finite Element Analysis, ed. by J. Bathe, et al., MIT Press, 1977, pp. 673-690.

5. Belytschko, T. and Mullen, R., "Stability of Explicit-Implicit Mesh Partitions in Time Integration," International Journal of Numerical Methods in Engineering, Vol. 12, 1978, pp. 1575-1586.

6. Hughes, T.J.R., and Liu, W.K., "Implicit-Explicit Finite Elements in Transient Analysis: Stability Theory," Journal of Applied Mechanics, Vol. 45, 1978, pp. 371-374.

7. Liu, W.K. and Belytschko, T., "Mixed Time Implicit-Explicit Finite Elements for Transient Analysis," Computers and Structures, Vol. 15, pp. 445-450, 1982.

8. Belytschko, T., Yen, H.J. and Mullen, R., "Mixed Methods for Time Integration," Computer Methods in Applied Mechanics and Engineering, Vol. 17, 1979, pp. 259-275.

9. Belytschko, T., "Partitioned and Adaptive Algorithms for Explicit Time Integration," U.S. - Europe Finite Element Seminar, Bochum, Germany, July 1980, in Nonlinear Finite Element Analysis in Structural Mechanics, ed. by W. Wunderlich, et al., 1980, pp. 572-584.

10. Belytschko, T. and Robinson, R.R., "SAMSON 2: A Nonlinear Two Dimensional Structure/Media Interaction Computer Code," Air Force Weapons Laboratory, Kirkland Air Force Base, New Mexico, November 1981, Report AFWL-TR-81-109.

11. Wright, J.P., "Mixed Time Integration Schemes," Computers and Structures, Vol. 10, 1979, pp. 235-238.

12. Belytschko, T., Ong, J., Liu, W.K. and Kennedy, J.M., "Hourglass Control in Linear and Nonlinear Problems," Computer Methods in Applied Mechanics and Engineering, Vol. 43, 1984, pp.251-276.

DISTRIBUTION LIST

No. of Copies	Organization	No. of Copies	Organization
12	Administrator Defense Technical Info Center ATTN: DTIC-FDAC Cameron Station, Bldg 5 Alexandria, VA 22304-6145	1	Commander US Army Materiel Command ATTN: AMCDRA-ST 5001 Eisenhower Avenue Alexandria, VA 22333-0001
1	Director Defense Advanced Research Projects Agency ATTN: Dr. W. Snowden 1400 Wilson Boulevard Arlington, VA 22209	2	Commander US Army Armament Research, Development and Engineering Center ATTN: SMCAR-LCU-CT E. Barrieres SMCAR-SCM Dr. E. Bloore Dover, NJ 07801-5001
1	Director Defense Nuclear Agency Washington, DC 20305	1	Commander US Army Armament Research, Development and Engineering Center ATTN: SMCAR-MSI Dover, NJ 07801-5001
1	Deputy Assistant Secretary of the Army (R&D) Department of the Army Washington, DC 20310		
1	HQDA (DAMA-ARP) Washington, DC 20310-2500	1	Commander US Army Armament Research, Development and Engineering Center ATTN: SMCAR-TDC Dover, NJ 07801-5001
1	HQDA (DAMA-ART-M) Washington, DC 20310-2500		
1	HQDA (DAMA-MS) Washington, DC 20310-2500		
2	Commander US Army BMD Advanced Technology Center ATTN: BMDATC-M, Mr. P. Boyd Mr. S. Brockway P.O. Box 1500 Huntsville, AL 35807-3801	2	Director US Army AMCCOM ARDEC CCAC Benet Weapons Laboratory ATTN: SLCAR-CCB-TL Dr. Joseph F. Flaherty Watervliet, NY 12189-4050
2	Director US Army Engineer Waterways Experiment Station ATTN: Dr. P. Hadala Dr. B. Rohani P.O. Box 631 Vicksburg, MS 39180-0631	1	Commander US Army Armament, Munitions and Chemical Command ATTN: SMCAR-IMP-L Rock Island, IL 61299-7300
		1	Commander US Army Aviation Systems Command ATTN: AMSAV-ES 4300 Goodfellow Blvd. St. Louis, MO 63120-1798

DISTRIBUTION LIST

No. of Copies	Organization	No. of Copies	Organization
1	Director US Army Aviation Research and Technology Activity Ames Research Center Moffett Field, CA 94035-1099	6	Director US Army Materials Technology Laboratory ATTN: SLCMT-D Mr. J. Mescall Dr. M. Lenoe R. Shea
1	Commander US Army Communications- Electronics Command ATTN: AMSEL-ED Fort Monmouth, NJ 07703-5301		F. Quigley SLCMT-ATL Watertown, MA 02172-0001
1	Commander CECOM R&D Technical Library ATTN: AMSEL-IM-L (Reports Section) B. 2700 Fort Monmouth, NJ 07703-5000	2	Commander US Army Research Office ATTN: SLCRO-MS, Dr. E. Saibel Dr. G. Mayer P.O. Box 12211 Research Triangle Park, NC 27709-2211
1	Commander US Army Missile Command ATTN: AMSMI-RD Redstone Arsenal, AL 35898-5245	1	Director US Army TRADOC Analysis Activity ATTN: ATOR-TSL White Sands Missile Range, NM 88002-5502
1	Commander US Army Missile Command ATTN: AMSMI-RX Redstone Arsenal, AL 35898-5249	1	Commandant US Army Infantry School ATTN: ATSH-CD-CS-OR Fort Benning, GA 31905-5400
1	Commander US Army Missile and Space Intelligence Center ATTN: AIAMS-YDL Redstone Arsenal, AL 35898-5500	1	Commander US Army Development and Employment Agency ATTN: MODE-ORO Fort Lewis, WA 98433-5000
3	Commander US Army Tank-Automotive Command ATTN: AMSTA-TSL V. H. Pagano T. Dean Warren, MI 48397-5000	1	Commander Naval Air Systems Command ATTN: AIR-604 Washington, DC 20360
		1	Commander Naval Air Development Center, Johnsville Warminster, PA 18974

32

DISTRIBUTION LIST

No. of Copies	Organization	No. of Copies	Organization
1	Commander Naval Sea Systems Command Department of the Navy ATTN: Code SEA 62D Washington, DC 20362-5101	3	Commander Naval Weapons Center ATTN: Code 31804, Mr. M. Smith Code 326, Mr. P. Cordle Code 3261, Mr. T. Zulkoski China Lake, CA 93555-6001
1	Commander Naval Missile Center Point Mugu, CA 93041		
2	Naval Ship Engineering Center ATTN: J. Schell Tech Lib Washington, DC 20362	7	Commander Naval Weapons Center ATTN: Code 3181, John Morrow Code 3261, Mr. C. Johnson Code 3171,
1	Commader David W. Taylor Naval Ship Research & Development Command ATTN: Code 1740.4, R. A. Gramm Bethesda, MD 20084-5000		M. B. Galloway Code 3831, Mr. M. Backman Dr. O. E. R Heimdahl Dr. Kenneth Graham Code 3894, C. Lorenzen China Lake, CA 93555-6001
2	Commander Naval Surface Weapons Center ATTN: Code G, Dr. W. G. Soper Mr. N. Rupert Code G35, D. Peterson Dahlgren, VA 22448-5000	1	Director Naval Research Laboratory ATTN: Dr. C. Sanday Washington, DC 20375
10	Commander Naval Surface Weapons Center ATTN: Code R-32 Alexander Rozner Hampton de Jarnette Code U-23 William Hinckley Code R-13, F. J. Zerilli K. Kim E. T. Toton M. J. Frankel Code U-11, J. R. Renzi R. S. Gross Code K-22, J. Etheridge Silver Spring, MD 20902-5000	3	Superintendent Naval Postgraduate School ATTN: Dir of Lib Dr. Gilbert Kinny Dr. Richard Reinhardt Monterey, CA 93940
		1	HQ USAF/SAMI Washington, DC 20330
		1	AFIS/INOT Washington, DC 20330
		3	ADTC/DLJW (LT K. Ols, LT J. Flores, Mr. W. Cook) Eglin AFB, FL 32542

DISTRIBUTION LIST

No. of Copies	Organization	No. of Copies	Organization
1	ADTC/DLYV (Mr. J. Collins) Eglin AFB, FL 32542	7	Director Los Alamos Scientific Laboratory
1	AFATL/DOIL (Tech Info Center) Eglin AFB, FL 32542-5438		ATTN: Dr. R. Karpp Dr. J. Dienes Dr. J. Taylor
1	AFWL-SUL Kirtland AB, NM 87117		John Meier Scott Hill Dr. C. Mader
1	AUL-LSE 71-249 Maxwell AFB, AL 36112		Tech Library P.O. Box 1663 Los Alamos, NM 87544
1	AFWAL/MLLN (Dr. T. Nicholas) Wright-Patterson AFB, OH 45433	9	Sandia National Laboratories ATTN: Dr. R. Woodfin Dr. M. Sears
1	Lawrence Livermore National Laboratory ATTN: Technical Library P.O. Box 808 Livermore, CA 94550-0622		Dr. W. Herrmann Dr. A. Chabai M. Kipp T. Burns A. L. Stevens M. J. Forrestal
1	Lawrence Livermore National Laboratory ATTN: Dr. J. O. Hallquist P.O. Box 808 Livermore, CA 94550-0622		M. J. Sagartz L. Davison P.O. Box 5800 Albuquerque, NM 87185-5800
1	Lawrence Livermore National Laboratory ATTN: Dr. M. L. Wilkins P.O. Box 808 Livermore, CA 94550-0622	2	Sandia National Laboratories ATTN: Dr. L. D. Bertholf Dr. D. Bammann P.O. Box 969 Livermore, CA 94550
1	Lawrence Livermore National Laboratory ATTN: Dr. G. Goudreau P.O. Box 808 Livermore, CA 94550-0622	1	Headquarters National Aeronautics and Space Administration Washington, DC 20546
		10	Central Intelligence Agency OIR/DB/Standard GE47 HQ Washington, DC 20505
		1	US Geological Survey 2255 N. Gemini Drive ATTN: Dr. D. Roddy Flagstaff, AZ 86001

DISTRIBUTION LIST

No. of Copies	Organization	No. of Copies	Organization
1	AAI Corporation ATTN: R. L. Kachinski P.O. Box 67 Baltimore, MD 21204	4	Ford Aerospace and Communications Corporation Ford Road, P.O. Box A ATTN: L. K. Goodwin C. E. Blair E. R. Mijares R. C. Morenus Newport Beach, CA 92660
1	AVCO Systems Division ATTN: Dr. Reinecke 201 Lowell Street Wilmington, MA 01803		
1	Battelle Columbus Laboratories ATTN: G. Throner 505 King Avenue Columbus, OH 43201	1	General Dynamics ATTN: J. H. Cuadros P.O. Box 2507 Pomona, CA 91766
4	Boeing Aerospace Company ATTN: Mr. R. G. Blaisdell (M.S. 40-25) Dr. N. A. Armstrong, C. J. Artura (M.S. 8C-23) Dr. B. J. Henderson (M.S. 43-12) Seattle, WA 98124	1	General Electric Company ATTN: D. Graham, Rm 1311 Lakeside Avenue Burlington, VT 05401
		1	H. P. White Laboratory 3114 Scarboro Road Street, MD 21154
		5	Honeywell, Inc. ATTN: Mr. J. Blackburn Dr. G. Johnson Mr. K. H.Doeringsfeld Dr. C. Candland Ms. Peggy Anderson 5901 South County Road 18 Edina, MN 55436
1	Computer Code Consultants, Incorporated ATTN: Dr. Wally Johnson 1680 Camino Redondo Los Alamos, NM 87544		
1	Electric Power Research Institute ATTN: Dr. Geore Sliter P.O. Box 10412 Palo Alto, CA 94303	1	Lockheed Missiles and Space Company ATTN: Org 8320, Bldg 157-3W Robert Weinheimer P.O. Box 3504 Sunnyvale, CA 94088-3504
4	FMC Corporation Ordnance Engineering Division ATTN: Neil Kennedy Claude Braafladt Robert Burt Anthony Lee P.O. Box 1201 San Jose, CA 95108	2	Lockheed Missiles and Space Company ATTN: R. L. Williams Dept 81-11, Bldg 154 Robert Cothern Dept 6-54, Bldg 153 P.O. Box 504 Sunnyvale, CA 94086

DISTRIBUTION LIST

No. of Copies	Organization	No. of Copies	Organization
1	Materials Research Laboratory, Inc. 1 Science Road Glenwood, IL 60427	3	Schumberger Well Services Perforating Center ATTN: J. E. Brooks J. Brookman Dr. C. Aseltine P.O. Box A Rosharon, TX 77543
2	McDonnell-Douglas Astronautics Company 5301 Bolsa Avenue ATTN: Dr. L. B. Greszczuk Dr. J. Wall Huntington Beach, CA 92647	6	Strategic Defense Initiative Organization ATTN: Dr. Gerold Jones, Rm 416 Dr. James Ionson, Rm 326 COL Malcolm O'Neill, Rm 734 Dr. Louis Marquet, Rm 331 Mr. John Gardner, Rm 332 COL George Hess, Rm 449 1717 H Street, NW Washington, DC 20006
3	New Mexico Institute of Mining and Technology ATTN: Lamar Kempton Dr. Max Bloom Dr. M. A. Meyer Socorro, N 87801		
2	Orlando Technology, Inc. ATTN: Mr. J. Osborne Mr. D. Matuska P.O. Box 855 Shalimar, FL 32579		
1	Pacific Technical Corporation ATTN: Dr. F. K. Feldmann 460 Ward Drive Santa Barbara, CA 93105	1	Systems, Science and Software ATTN Dr. R. Sedgwick P.O. Box 1620 La Jolla, CA 92037
1	Rockwell International Missile Systems Division ATTN: A. R. Glaser 4300 E. Fifth Avenue Columbus, OH 43216	2	TRW One Space Park, R1/2120 ATTN: D. Ausherman M. Bronstein Redondo Beach, CA 90277
4	SRI International ATTN: Dr. L. Seaman Dr. L. Curran Dr. D. Shockey Dr. A. L. Florence 333 Ravenswood Avenue Menlo Park, CA 94025-3493	1	United Technologies Research Center ATTN: P. R. Fitzpatrick 438 Weir Street Glastonbury, CT 06033

DISTRIBUTION LIST

No. of Copies	Organization	No. of Copies	Organization
2	LTV Aerospace and Defense Company Vought Missiles and Advanced Programs Division ATTN: Dr. G. Hough Dr. Paul M. Kenner P.O. Box 650003 Dallas, TX 75265-0003	4	University of Delaware Department of Mechanical Engineering ATN: Prof. J. Vinson Prof. B. Pipes Prof. M. Taya Prof. T-Y Chou Newark, DE 19711
1	US Steel Corporation Research Center 125 Jamison Center Monroeville, PA 15146	1	University of Denver Denver Research Institute ATTN: Mr. R. F. Recht 2390 S. University Bld. Denver, CO 80210
4	Southwest Research Institute Dept. of Mechanical Sciences ATTN: Dr. U. Lindholm Dr. R. White Dr. M. F. Kanninen Dr. C. Anderson 8500 Culebra Road San Antonio, TX 78228	1	University of Florida Department of Engineering Sciences ATTN: Dr. L. E. Malvern Gainesville, FL 32601
1	Drexel University Department of Mechanical Engr. ATTN: Dr. P. C. Chou 32d and Chestnut Streets Philadelphia, PA 19104		Aberdeen Proving Ground Dir, USAMSAA ATTN: AMXSY-D AMXSY-MP, H. Cohen Cdr, USATECOM ATTN: AMSTE-SI-F
2	University of Arizona Civil Engineering Department ATTN: Dr. D. A. DaDeppo Dr. R. Richard Tucson, AZ 85721		Dir, USA CSTA ATTN: Mr. W. Pless Mr. S. Keithley Cdr, CRDC, AMCCOM ATTN: SMCCR-RSP-A SMCCR-MU
2	University of California College of Engineering ATTN: Prof. W. Goldsmith Dr. A. G. Evans Berkeley, CA 94720		SMCCR-SPS-IL

USER EVALUATION SHEET/CHANGE OF ADDRESS

This Laboratory undertakes a continuing effort to improve the quality of the reports it publishes. Your comments/answers to the items/questions below will aid us in our efforts.

1. BRL Report Number_____Date of Report_____

2. Date Report Received_____

3. Does this report satisfy a need? (Comment on purpose, related project, or other area of interest for which the report will be used.)_____

_____

_____

4. How specifically, is the report being used? (Information source, design data, procedure, source of ideas, etc.)_____

_____

_____

5. Has the information in this report led to any quantitative savings as far as man-hours or dollars saved, operating costs avoided or efficiencies achieved, etc? If so, please elaborate._____

_____

_____

6. General Comments. What do you think should be changed to improve future reports? (Indicate changes to organization, technical content, format, etc.)

_____

_____

_____

CURRENT
ADDRESS

Name _____

Organization _____

Address _____

City, State, Zip _____

7. If indicating a Change of Address or Address Correction, please provide the New or Correct Address in Block 6 above and the Old or Incorrect address below.

OLD
ADDRESS

Name _____

Organization _____

Address _____

City, State, Zip _____

(Remove this sheet, fold as indicated, staple or tape closed, and mail.)

END

9-87

DTIC